KfK 4657
Februar 1990

Temperature and Stress Analysis of the Self-cooled DEMO Liquid Metal Blanket (Option A)

P. Norajitra
Institut für Material- und Festkörperforschung
Projekt Kernfusion

Kernforschungszentrum Karlsruhe

KERNFORSCHUNGSZENTRUM KARLSRUHE GmbH
Institut für Material- und Festkörperforschung
Projekt Kernfusion

KfK 4657

Temperature and Stress Analysis of the Self-cooled DEMO Liquid Metal Blanket (Option A)

P. Norajitra

Kernforschungszentrum Karlsruhe GmbH, Karlsruhe

Kernforschungszentrum Karlsruhe GmbH
Postfach 3640, 7500 Karlsruhe 1

ISSN 0303-4003

Zusammenfassung:

Temperatur- und Spannungsanalyse für das selbstgekühlte DEMO-Flüssigmetallblanket (Option A)

Im Rahmen der DEMO-Brutblanketentwicklung wird im KfK unter anderem das Konzept eines selbstgekühlten Flüssigmetallblankets verfolgt. Gegenstand dieses Berichtes sind die Temperatur- und Spannungsrechnungen zur ersten Konzeptvariante (Option A), bei der sich das Brutblanket mit Beryllium als Multiplier nur auf der Outboardseite befindet.

Die Temperatur- und Spannungsrechnungen wurden für den stationären Betrieb, mit Hilfe des Finite-Element-Programmes ABAQUS, zweidimensional durchgeführt. Betrachtet wurde der dem Plasma zugewandte vordere Blanketteil (Multiplierregion) im Bereich der thermisch höchstbelasteten Blanketmittelebene. Die Belastungsrandbedingungen wurden konservativ angenommen, und zwar mit einem Spitzenwert der Oberflächenwärmebelastung von 50 W/cm2 und einem maximalen Blanketinnendruck von 50 bar. Außerdem wurde die konservative Annahme getroffen, daß die maximale Innendruckbelastung und die maximale thermische Belastung in derselben Blanketebene auftreten.

Das Ergebnis der Temperaturrechnung zeigt, daß alle Temperaturen unterhalb der gewünschten Auslegungsgrenzen liegen. Die maximale Temperatur wurde in der Ersten Wand mit 530 °C und im Beryllium mit 495 °C ermittelt. Dabei erweist sich die mäanderförmige Strömungskanalführung in der Multiplierregion als optimal. Die Spannungsrechnungen wurden zweidimensional linear-elastisch durchgeführt. Die Beurteilung der Spannungen erfolgt nach dem ASME-Code. Das Ergebnis dieser Analyse zeigt, daß alle Spannungen trotz der konservativ getroffenen Annahmen noch beträchtlich unterhalb der zulässigen Grenzwerte liegen.

Abstract

Within the framework of DEMO breeder blanket development the concept of a self-cooled liquid metal blanket is pursued among others at KfK. This report is an account of the temperature and stress computations on the first concept variant (option A) in which the breeder blanket with beryllium as neutron multiplier is provided exclusively on the outboard side.

The temperature and stress computations were performed two-dimensionally for steady-state operation using the ABAQUS finite element code. The blanket mid-plane undergoing maximum thermal loading of the plasma facing front part of the blanket (multiplier region) was considered. A conservative assumption was made in respect of the boundary conditions of loading, with a peak value of the surface heat load of 50 W/cm^2 and a maximum blanket internal pressure of 50bar. Besides, the conservative assumption was made that the maximum loading by internal pressure and the maximum thermal loading occur in the same blanket plane.

The result of temperature computation shows that all temperatures remain below the desired design limits. The maximum temperature of the first wall was determined to be 530 °C and of beryllium to be 495 °C. The meander shaped routing of the flow channel in the multiplier region proves to be optimal. The stress calculations were made two-dimensionally, linearly elastically. The stresses were evaluated using the ASME code. The result of this analysis shows that all stresses, despite of the conservative assumptions made, are still well below the admissible limits.

Table of Contents

1 Introduction

Within the framework of breeder blanket development for the DEMO power reactor the blanket concept involving liquid metal cooling has been pursued at KfK for some time [1]. The essential tasks of a breeder blanket consists in breeding the tritium needed for reactor operation, in transforming the neutron kinetic energy into heat at a temperature level favorable to electricity generation, and in shielding the magnets from radiation. The liquid metal consisting of an eutectic lead-lithium alloy (83Pb-17Li) which is used in the breeder blanket serves as the breeder material and, at the same time, as the coolant. Such a blanket concept is called a "self-cooled blanket".

The many advantages resulting from the use of liquid metal as the breeder and coolant are counteracted, however, by serious problems associated with magnetohydrodanymics (MHD). They are due mainly to the influence exerted by the strong magnetic field on the flowing liquid metal. The basic prerequisite of the feasibility of a liquid metal cooled blanket is therefore flow routing optimized under MHD aspects. To minimize the pressure drops and hence the mechanical stress, the velocity normal to the magnetic field must be as low as possible. Higher coolant velocities are admissible only in the channels running parallel to the magnetic field. The blanket concept described below relies on this principle of flow routing.

Two variants of the self-cooled blanket concept (Figure 1) are eligible [2], namely the concept of a breeder blanket provided exclusively in the outboard which needs sufficient beryllium as the neutron multiplier (option A) and the concept of a breeder blanket provided in the inboard and in the outboard without any beryllium (option B). At present, development work is concentrating on option A. Doing without an inboard blanket under this option offers adavantages because the magnetic field causing the MHD pressure losses is by about 50 % more intense in the inboard than in the outboard. Under this concept, the coolant piping, similar to all the rest of blanket concepts considered within the EC, is routed from top into the torus.

This report is an account of the temperature and stress computations. The central activities are the thermal hydraulic design of the blanket, the optimization of the static first wall load and of the beryllium temperature as well as the verification of static loading of the blanket structure in the zone of maximum thermal loading. The computations relating to steady-state operation are made two-dimensionally with the finite elemente code ABAQUS [3]. Further three-dimensional computations are planned.

2 Layout of a Liquid Metal Blanket

Figure 2 shows the general layout of a self-cooled liquid metal blanket and Figure 3 its cross-section through the blanket midplane. The coolant enters the rear channels of the blanket box via pipes of large cross-sections, flows downward and is reversed by 180° into channels, which are confined by inclined baffle plates. These baffle plates push gradually all the coolant through the beryllium zone during upward flow. In the beryllium zone the coolant initially flows at relatively high velocity through a narrow gap between the beryllium plates and the first wall exposed to high thermal loading and is then routed in a meander through two coolant channels provided in the beryllium where it is further heated. The hot lead-lithium now reflows into the blanket mid-zone where it is again rerouted upwards in direction of the outlet.

The blanket box is made of martensitic steel 1.4914 (EC designation MANET). It has an almost rectangular cross-section (Figure 3) and is provided with bracings so as to withstand high pressure as much as possible.

The critical part of the blanket segment is the first wall, which separates the liquid metal system from the plasma space. Besides a high loading by internal coolant pressure it is locally exposed to high thermal loading caused by α-particles and neutron radiation originating from the plasma. To achieve the greatest possible strength of the first wall the latter is given a corrugated shape and welded to a stiffening plate between two corrugations each. These numerous partitioning walls produce the effect that the whole front part of the blanket in the beryllium zone makes up an inherently stiff body. The beryllium is placed between the first wall supporting plates or webs (Figure 2). In the beryllium plates meander shaped coolant channels run which guarantee optimum cooling. In Figure 3 the beryllium plates have not been sketched for better transparency.

In the blanket segment the coolant flows at velocities between about 0.7 m/s (in the rear channels across the magnetic field) and 2 m/s (along the first wall parallel to the major magnetic field). By this type of flow routing the MHD pressure drops can be kept minimum as already mentioned. To avoid further MHD pressure drops by electric short circuit currents in the supporting structures flow channel inserts are used which consist of a double sheet metal and a thin electrically insulating ceramic intermediate layer [4]. For the same purpose, the beryllium plates are provided with an electrically insulation layer and an external sheet metal coating.

3 Thermalhydraulic Design

The thermalhydraulic design of the liquid metal blanket is governed by the distribution of heat sources determined for this blanket design [5]. Accordingly, the total thermal power to be removed from the blanket is 38.2 MW, 4 MW of them thermal power on the surface. The required lead-lithium mass flow is determined from the power of the blanket segment and the maximum possible overall temperature rise. The latter is limited by the maximum admissible interface temperature between the steel and the liquid metal which is determined by corrosion. It is about 470 to 500 °C for the MANET steel so that the mean outlet temperature of lead-lithium of 400 °C can be taken as the basis. Considering the melting point of the eutectic alloy 83Pb-17Li of 235 °C the selected inlet temperature is 275 °C. This gives a total temperature rise of 125 K and a total coolant mass flow through the blanket segment of 1617 kg/s.

In thermalhydraulic design also the criteria apply that the temperature of the first wall, due to creep rupture strength, must not exceed the maximum of about 550 °C and the beryllium temperature, on account of neutron induced swelling, must not go beyond the maximum of 500 °C. An optimum design is achieved if in all front channels of the blanket segment the same temperature rise is set. In conformity with the poloidal power distribution (Figure 6), the coolant mass flow of a cell according to Figure 4 is 21 kg/s in the center of the blanket. The total number of cells over the total height of the blanket is taken as 96.

From the coolant flow and the coolant channel cross-section (channel I: 11.1 cm^2, channels II and III: 16.8 cm^2) a coolant velocity of 2 m/s is obtained for the first wall coolant channel (I) and of 1.3 m/s, respectively, for the beryllium coolant channels (II, III).

In Table 1 the general design data for the DEMO liquid metal blanket have been compiled. The MHD pressure drops and the absolute pressures as a function of the level of installation of the liquid metal pump in the blanket coolant circuit have been estimated in [6]. The values indicated apply to the least favorable case of a high level of pump installation. The maximum internal pressure of the blanket of 50 bar is not the result of MHD pressure drop calculations, but conforms to the desire to have the largest possible "window" for MHD multichannel pressure drops which cannot be quantified now.

The mean coolant temperature and coolant pressure distributions in the blanket have been represented in Figure 5. The coolant enters at 275 °C and initially is

heated but slightly by 1.5 K on its downward flow. After it has been rerouted at the bottom it is heated up to a temperature value of approximately 284 °C during upward flow until it enters the first wall coolant channel in the midplane of the blanket. Subsequently, the coolant is considerably heated up while it flows through the multiplier region. At a temperature just below 400 °C it leaves the front blanket zone and flows together with the other partial coolant flows upwards to the outlet where the mean coolant mixing temperature attains the value of 400 °C.

4 Computation of the Temperature Distribution

4.1 Geometry

Figure 4 shows a section through the multiplier region of the geometric model of a cell in a computer readable representation. For the construction of the finite element (FE) structure the FEMGEN code [7] is referred to. In conformity with the radial power distribution the FE structure is more finely distibuted in the front part as compared with the rear part. The 6 mm thick first wall has been given a corrugated shape in order to releave it from the thermal load and to attain the maximum possible strength. This geometry was determined by optimizing calculations performed in parallel. The thickness of the first wall, the web spacing, and the shape of the profile of the first wall were subjected to variations. Reducing the thickness of the first wall causes e.g. a decrease in thermal stress, but at the same time a rise in primary stress. A more vaulted shape of the profile of the first wall would releave it even more from thermal stress, but, on the other hand, make fabrication more complicated and more expensive. Given the neutron physics requirements with respect to the tritium breeding ratio, the thickness of the webs has been reduced to the minimum. Shortening the web spacing contributes to stress relief in the webs and to lower beryllium temperatures, but makes more difficult access for welding operations during fabrication. The compromise found is the present geometry.

Beryllium, which is surrounded by an 0.5 mm thick metal sheet, lies between the web walls with a lateral gap of 0.5 mm. The lead-lithium contained in it is considered stagnant.

4.2 Power Distribution

Figure 6 shows the poloidal power distribution in the multiplier region. In calculating the power [5] the blanket was divided into 20 poloidal segments of 5.725° each. Each division corresponds roughly to five cells according to Figure 4. Thus, the cell power in the center of the blanket is twice that at the two blanket ends.

The radial distribution of the power density in steel, beryllium and Pb-17Li is represented in Figure 7. The exponential development in steel and beryllium can be well recognized. The maximum for steel is 20 W/cm^3 in the first wall and for beryllium 16 W/cm^3. The plot for lead-lithium is different. The maximum of 52 W/cm^3 of coolant channel II occurs in the beryllium zone. In coolant channel I at the first wall and channel III in beryllium zone, the values are 32 W/cm^3 and 26 W/cm^3, respectively. Most of the power release takes place in the front blanket region (mulitplier region). In the blanket regions behind, the thermal power is neglibly low so that coolant heating up in the poloidal coolant channels is accordingly low (Figure 5).

The surface heat flux introduced by the plasma is 40 W/cm^2 on the average. However, in the present computation a peak value of 50 W/cm^2 is adopted in a conservative assumption.

4.3 Material Data, Heat Transfer Coefficient

The thermal conductivity of lead-lithium, MANET steel and beryllium have been entered in Table 2 as a function of the temperature. Different from beryllium, the thermal conductivity of lead-lithium and steel increases with increasing temperature. At 500 °C the value for lead-lithium is e.g. 17 W/mK, for steel 26 W/mK, and for beryllium 95 W/mK. The specific heat capacity c_p of lead-lithium is 189 J/kgK in the temperature range of 300 to 500 °C. The density of lead-lithium is 9490 kg/m^3 at 300 °C and 9190 kg/m^3 at 500 °C, respectively.

The heat transport between beryllium and the coolant is deteriorated by the electrically insulating layer applied. This is taken into account by a heat transfer coefficient of 1 W/cm^{2}K. The value corresponds to a heat transfer ratio in fresh fuel pins for fast breeder reactors [12] with a nearly closed gap.

4.4 Method of Computation

While it passes the multiplier region, lead-lithium must absorb, besides its own high heat source, a considerable amount of heat from the surrounding structures. Due to the high heat flux and the relatively poor thermal conductivity of lead-lithium steep temperature gradients develop quickly in this flowing liquid metal across the flow direction. The temperature level and the temperature distribution in the solid structural parts are greatly influenced by this. Therefore, knowledge of the temperature distribution is of major importance both in liquid metal and in the structural parts.

Because of the lack of more sophisticated computer programs for the combined application to solids and fluids, the method of a moving coordinate system has been utilized for the computation. Quasi non steady-state computations are made within the calculated transit time of the fluid, with the specific heat of the solid portions set zero. The transit time or residence time of the fluid is determined from the known coolant channel length and coolant velocity, and for the first wall coolant channel it is 0.57 s and 0.86 s, respectively, for the beryllium coolant channels II and III.

The different flow directions require in addition that the temperatures of some sub-regions are calculated separately in an initial step and that after averaging of the temperatures at the points of separation, the computation is repeated. This applies also to the connection with the rear box part with the poloidal inlet channels.

For reasons inherent in computation some simplifying assumptions must be made. These are:

a) The flow velocity in the coolant channels is evenly distributed over the entire cross-section and has no component normal to the flow direction. This means that there is no cross mixing of flow. Consequently, the heat across the flow direction is transported solely by thermal conduction. This assumption of so-called slug flow applies approximately to MHD induced liquid metal flows.

b) Channel bending in beryllium is fictitiously replaced by two straight channels. Their temperature distribution at the point of transition is mirror symmetric. Seen in the direction of flow, this is the transition from channel II to channel III.

c) The coolant temperature at the inlet of the coolant channels I and II is homogeneously distributed over the cross-section, if almost complete flow mixing is assumed.

d) The axial heat transport by conductivity in direction of flow is neglected.

4.5 Result of the Temperature Computation

In Figure 8 the calculated temperature distribution in the multiplier region has been represented for the coolant inlet and outlet planes. The details of temperature distribution in the coolant, at the end of the meander shaped coolant channels I, II and III, are evident from Figures 9 to 11. The temperature distributions are represented as isotherms. At the respective end of the coolant channel relatively dense families of curves can be recognized, especially in the near range of the first wall in coolant channel I. The first wall temperature here is 530 °C at the maximum. The coolant temperature rise is 41 K for the first wall coolant channel. This corresponds to 163 kW heat removal, 60 kW (≙ 37 %) of it being power generated in the first wall (surface power plus volumetric power). The ratio of surface power to volumetric power of the first wall is about 4:1. In Table 3 the power balance is given for all three subchannels. A relatively high power contribution by lead-lithium of about 42 % of the total power gets evident. Corresponding to the position of the power maximum in lead-lithium (Figure 7), a relatively high coolant temperature rise of 49 K is obtained for the beryllium coolant channel II. This leads to a maximum beryllium temperature of 495 °C at the end of channel II. In the rear beryllium coolant channel III the temperature rise is still only 22 K on account of the lower power. The mean coolant outlet temperature at the end of channel III is 396 °C. Due to the better heat balance between the hot and the cold coolant, the temperature in beryllium is rather uniformly distributed. The temperature at the interface between the steel wall and liquid metal flow is 445 °C at the maximum there. In the gap filled with stagnant lead-lithium an absolute maximum of the interface temperature of 500 °C can be determined at the end of the channel II. The mean temperature of the rear intermediate plate is between 400 °C at the coolant entrance level and 450 °C at the coolant outlet level.

These are the important maximum values:

- maximum first wall temperature:
  - . inside 404 °C
  - . outside 530 °C
- maximum beryllium temperature: 495 °C

- maximum temperature at the steel/coolant interface:
  - . in the coolant channel 445 °C
  - . in the stagnant Pb-17Li-gap 500 °C

In Figure 12 through 14 radial, poloidal and toroidal temperature plots in the multiplier region have been represented as examples. The points of temperature maxima have been marked.

Figure 15 shows the temperature distribution in the equatorial cross-section of the blanket. The "cold" and "hot" regions in the blanket can be recognized; they differ from each other by dark and light shades. On account of little power released, only little temperature differences can be observed across the walls in the rear box zone. At the main diagonal baffle plate which separates the cold coolant from the hot coolant, a maximum difference of the wall temperature of 60 K can be measured.

In Table 4 the temperatures and liquid metal mass flows have been compiled for three blanket planes with the temperares for blanket ends estimated in an approximation using the ratio of power densities. It is visible from this estimation that the maximum thermal loading of the structure occurs in the center of the blanket and the maximum loading of the structure by internal pressure at the lower end of the blanket.

5 Stress Computation

5.1 Geometry

In Figure 16 the used finite element model of the front blanket structure has been represented as a radial blanket segment of about 6°. The selected blanket section with five structural cells roughly corresponds to the zone of maximum thermal loading in the center of the blanket (see Figure 6).

For two-dimensional stress computation using the ABAQUS code an element of the continuum generalized plane strain element type is used which allows to record simultaneously the stresses quasi three-dimensionally which are generated in toroidal direction by differential thermal expansions. This is done by the integrated boundary condition that the parallel planes of computation and control remain plane. This boundary condition is used in the computation for the

sectional planes as well. Besides on the temperature distributions determined in the structure around the blanket center (Figure 17), the computations are based on a maximum of 50 bar loading by internal pressure. Moreover, the conservative assumption is made that the maximum loading by internal pressure and the maximum thermal stresses occur in the same blanket cross-section although the maximum internal pressure gets effective at the lower end of the segment whereas the maximum thermal stresses act in the center of the torus.

5.2 Material Data and Admissible Load Limit

The envisaged structural material for the DEMO reactor is ferritic martensitic steel 1.4914 (MANET). It is characterized by a high strength, a higher thermal shock resistance, and a better swelling behaviour compared to austenitic steel (316L). Drawbacks are the more complicated fabrication and the shift in the ductile-brittle-transition temperature (DBTT) of the MANET steel exposed to radiation to a considerably higher value which defines a minimum operating temperature of the structural parts of 250 °C.

In Table 5 the strength values and the thermal expansion coefficient of MANET steel have been represented as a function of the temperature. The relatively low thermal expansion coefficient and the relatively high thermal conductivity are favorable to the behaviour of thermal stresses which is described by the thermal stress factor σ_T [MPa·m/W] $= \alpha \cdot E / \lambda(1-\nu)$, where α[1/K] is the thermal expansion coefficient, E [MPa] is the Young's modulus, λ[W/mK] is the thermal conductivity, and ν is the Poisson's ratio.

For evaluation of the stresses the regulations contained in the ASME code apply [13], [14]:

$\sigma_{adm} = 1 \cdot S_{m,t}$ for primary membrane stresses ($\sigma_{p.m}$), averaged over the cross-section

$\sigma_{adm} = 1.5 \cdot S_{m,t}$ for primary membrane plus bending stresses ($\sigma_{p.m+b}$)

$\sigma_{adm} = 3 \cdot S_m$ for primary and secondary stresses ($\sigma_{p.m+b} + \sigma_{sec}$)

with $S_m = \min(\frac{2}{3} \cdot \sigma_{0.2}, \frac{1}{3} \cdot \sigma_u)$ and $S_{m,t} = \min(S_m, \frac{2}{3} \cdot \sigma_{R,t}, 1 \cdot \sigma_{1,t})$.

$\sigma_{0.2}$ is the 0.2 % offset yield stress, σ_u is the ultimate tensile strength, $\sigma_{R,t}$ is the stress to cause creep rupture in time t, $\sigma_{1,t}$ is the stress to produce 1 % total strain

in time t. $t = 2 \cdot 10^4$ h for steady state operation of DEMO. The equivalent stress intensity used in the comparison with the admissible stress (σ_{adm}) is the von Mises stress derived according to the yielding criterion:

$$\sigma_{v,Mises} = \sqrt{\frac{(\sigma_1-\sigma_2)^2 + (\sigma_2-\sigma_3)^2 + (\sigma_3-\sigma_1)^2}{2}}$$

where σ_1, σ_2, σ_3 , are the principal stresses. The superposition of primary and secondary stresses is performed at the stress-component level.

The dependence on temperature and time to failure of the strength characteristic value S_m is obvious from Table 6. For a DEMO typical operation time of 2×10^4 h the S_m value decreases considerably above 500 °C. At a maximum design temperature of the first wall of 550 °C it is 98 MPa.

5.3 Result of Stress Computation

Table 6 shows the von Mises equivalent stresses in the load cases internal pressure (primary) and internal pressure plus temperature (primary + secondary) for the points marked in Figure 16. At these points under consideration the local temperature ϑ, the admissible limit values corresponding to that temperature σ_{adm}, and the margin between the actual stress and the admissible limit $\Delta\sigma$ are entered in addition. The stresses indicated in the table were calculated for 50 bar internal pressure. The result in the internal pressure load case shows that the margin $\Delta\sigma$ in the front part of the web plate exposed to tensile stress is minimum at the coolant inlet plane. At that point the primary membrane stress is 103 MPa at 502 °C. After linear extrapolation at about 65 bar internal pressure the limit value would be attained here. The first wall and the rear intermediate plate are exposed to tensile and bending stresses. The latter are even substantially intensified in the superimposed load case internal pressure plus temperature due to large temperature differences in the wall and in the structural parts.

In Figure 18 the development of normal stresses σ_{xx} and σ_{zz} (x $\hat{=}$ poloidal, z $\hat{=}$ toroidal) in the first wall is represented for the zone of maximum loading (section A-A, Figure 16). It can be recognized well that the external side of the first wall is subjected to compressive stress due to the higher temperature, whereas the inner side is subjected to tensile stress due to direct cooling. The portion of temperature bending stress which in the superimposed load case dominates over

the primary load case can likewise be clearly recognized. Furthermore, a relatively large stress portion can be recognized in toroidal (z) direction which is caused by the differential thermal expansions of the components in flow direction. The secondary stresses are very dominating in the first wall region which is likewise evident from the result in Table 6. At the point of the first wall undergoing maximum thermal loading, i.e. the external side of the first wall at the outlet of the first wall coolant channel in the midplane of the blanket (point 1, Figure 16), the distance $\Delta\sigma$ of 173 MPa between the axtual stress and the admissible stress is minimum. The stress at that point is 283 MPa at a maximum temperature of 530 °C. The distribution of stress intensity in this first wall region is evident from Figure 19. The stress is even higher on the inner side of the first wall, namely 319 MPa, which, however, provides an even greater safety margin with respect to the admissible value on account of the lower wall temperature of 404 °C. Another point with relatively little distance $\Delta\sigma$ from the admissible value lies in the web (point 5). However, the stress at this point would considerably decrease at a lower real internal pressure of the blanket because the fraction of primary stress in total stress is much higher here than in the first wall. A maximum shear stress at the point connecting the NaK pipe with the first wall is 137 MPa. The stresses determined are below the 0.2 % yield stress. Thermal ratchetting can be exlcuded because the $3 \cdot S_m$ limit values are observed. The maximum deformation of the multiplier structure in the center of the blanket is about 2.1 mm radially per cell and about 0.5 mm poloidally per cell.

Acknowledgements

This work has been performed in the framework of the Nuclear Fusion Project of the Kernforschungszentrum Karlsruhe and is supported by the European Communities within the European Fusion Technology Program.

6 References

[1] S. Malang, et al.
Self-cooled Liquid-Metal Blanket Concept
Fusion Technology, Vol. 14, November 1988, p.1343

[2] S. Malang, et al.
Test module in NET for a self-cooled liquid metal blanket concept
Proc. of the 15th Symp. on Fus. Techn., Utrecht, NL, September 19-23, 1988,
Amsterdam: North-Holland 1989, Vol. 2, S.1223-28

[3] ABAQUS User's Manual, 1988, Version 4.7
Hibbit, Karlsson & Sorensen Inc., Providence, Rhode Island

[4] L. Barleon, et al.
Untersuchung der magnetohydrodynamischen Strömungsvorgänge in den Kanälen eines selbstgekühlten Flüssigmetallblankets für NET
Das MEKKA-Programm
Jahrestagung Kerntechnik '89, Düsseldorf, 9.-11. Mai 1989,
Bonn: INFORUM 1989, S.621-624

[5] U. Fischer
March 1989, unpublished

[6] R. Möller
Internal KfK-Note, September 1989, unpublished

[7] FEMGEN Version 8.5, 1984
User Manual
FEGS Ltd., Oakington Cambridge

[8] U. Jauch, G. Haase, V. Karcher, B. Schulz
Thermophysical Properties in the System Li-Pb
KfK 4144, September 1986

[9] Blanket Advisory Group, KfK, compiled by M. Küchle
November 1988, unpublished

[10] N.P. Pinto, Chapter 16 "Properties" in "Beryllium Science and Technology"
Vol. 2, edited by D.R. Floyd and J.N. Lowe Plenum Press 1979

[11] K. Ehrlich
Internal KfK-Note, May 1986, unpublished

[12] K. Laßmann
Zum Wärmedurchgang im Bereich zwischen Hülle und Brennstoff eines Brennstabes.
Wärme- und Stoffübertragung 12 (1979), S. 185-202

[13] ASME Code III, edition 1986

[14] E. Zolti, et al.
Interim Structural Design Criteria for Predesign of the NET Plasma Facing Components
NET / IN / 86-14, March 1986

Table 1: General design data for the DEMO liquid metal blanket

Segment width, center	/m/	1.25
Poloidal segment length	/m/	8.7
Surface heat load	/W/cm^2/	
- mean value		40
- peak value		50
Segment power	/MW/	
- volumetric power		34.2
- surface power		4.0
- total power		38.2
Multiplier region		
- radial dimension	/mm/	320
- beryllium fraction		0.80
- steel fraction		0.07
- Pb-17Li-fraction		0.13
- theoretical tritium breeding ratio		1.05
Coolant		
- mass flow	/kg/s/	1617
- inlet temperature	/°C/	275
- outlet temperature	/°C/	400
- temperature rise	/K/	
. segment		125
. multiplier region		112
- velocity, maximum	/m/s/	
. front channels (first wall)		2
- MHD pressure drop, maximum	/bar/	
. front channels		about 5
. segment		about 25
- maximum absolute pressure	/bar/	50

Table 2: Thermal conductivity λ [W/mK]

Material	Temperature [°C]							Source
	20	100	200	300	400	500	600	
Pb-17 Li	(26.3)*	(28.7)*	(31.6)*	13.2	15.1	17.1	19.1	[8]
Steel 1.4914	24.2	24.7	25.2	25.6	25.9	26.2	26.4	[9], [11]
Beryllium	188	155	132	115	103	95	89	[10]

*) solid state (melting point: 235 °C)

Table 3: Power balance for the coolant channels at the equatorial plane (coolant mass flow $\dot{m}$ = 21 kg/s)

Channel	cross-section [cm²]	Velocity [m/s]	Coolant temperature [°C]		Bulk temperature rise [K]	Thermal power removal [kW]				
			inlet	oulet		FW	Be	Steel	Pb-Li	**Total**
I (First wall)	11.14	2.0	284	325	41	59.6	61.2	2.8	39.3	162.9
II (Beryllium)	16.80	1.3	325	374	49	-	94.6	2.8	97.3	194.7
III (Beryllium)	16.80	1.3	374	396	22	-	35.0	1.2	52.0	88.2

Total: 445.8 kW

Table 4: Temperature and pressure distributions at the three blanket levels

		Bottom	Center	Top
Coolant inlet temperature	[°C]	280	284	287
Liquid metal mass flow	[kg/s]	10,5	21	10,5
Maximum FW temperature	[°C]			
- inside		393	404	400
- outside		510	530	518
Maximum beryllium temperature	[°C]	446	495	453
Absolute pressure (maximum in the front part)	[bar]	48	39	29

Table 5: Material data for steel 1.4914 (MANET) [9], [11]

ϑ [°C]	E $\cdot 10^3$ [MPa]	v [-]	α / 20°C $\cdot 10^{-6}$ [1/K]	$\sigma_{0.2}$ 1) [MPa]	σ_u 2) [MPa]	S_m [MPa]	$S_{m,2\cdot 10^4 h}$ [MPa]
20	217	0.27	10.11	614	773	258	258
50	215	0.27	10.23	619	773	258	258
100	213	0.28	10.46	623	767	256	256
150	209	0.28	10.70	621	755	252	252
200	206	0.28	10.95	612	737	246	246
250	202	0.28	11.20	597	712	237	237
300	199	0.28	11.45	575	681	227	227
350	195	0.29	11.68	548	644	215	215
400	190	0.29	11.90	513	600	200	200
450	186	0.30	12.09	473	550	183	183
500	181	0.30	12.24	426	494	165	135
550	176	0.30	12.34	373	431	144	98
600	171	0.31	12.40	313	362	121	41

1) correponds to the designation $R_{p0.2}$ according to DIN 50145

2) corresponds to the designation R_m according to DIN 50145

Table 6: Von Mises equivalent stress of some characteristic highly loaded points, according to Figure 16

Point	Component	Reference Temperature		Dominant Type of Loading 2)	Primary Stress (p = 50 bar)			Primary plus Secondary Stress		
		ϑ [°C]	Plane 1)		$\sigma_{v.\ Mises}$ [MPa]	σ_{adm} [MPa]	$\Delta\sigma$ [MPa]	$\sigma_{v.\ Mises}$ [MPa]	σ_{adm} [MPa]	$\Delta\sigma$ [MPa]
1	First wall, outside	530	A	-, b	29	169	140	283	456	173
2 (2')	First wall, outside	481	A	-, b	146 (pt.2')	227	81	228	515	287
3	First wall, inside	404	A	+, b	129	298	169	319	596	277
4	NaK pipe connection	350	A	+, b,S	206	322	116	302	644	342
5	web	502	E	+	103	134	31	313	491	178
6	web	464	A	+	122	170	48	135	534	399
7	Intermediate plate	455	A	+, b	133	268	135	126	545	419
8	Intermediate plate	442	A	+, b	140	279	139	166	558	392

1) E = coolant inlet plane
A = coolant outlet plane

2) + = tensile stress
− = compressive stress
S = shear stress
b = bending stress

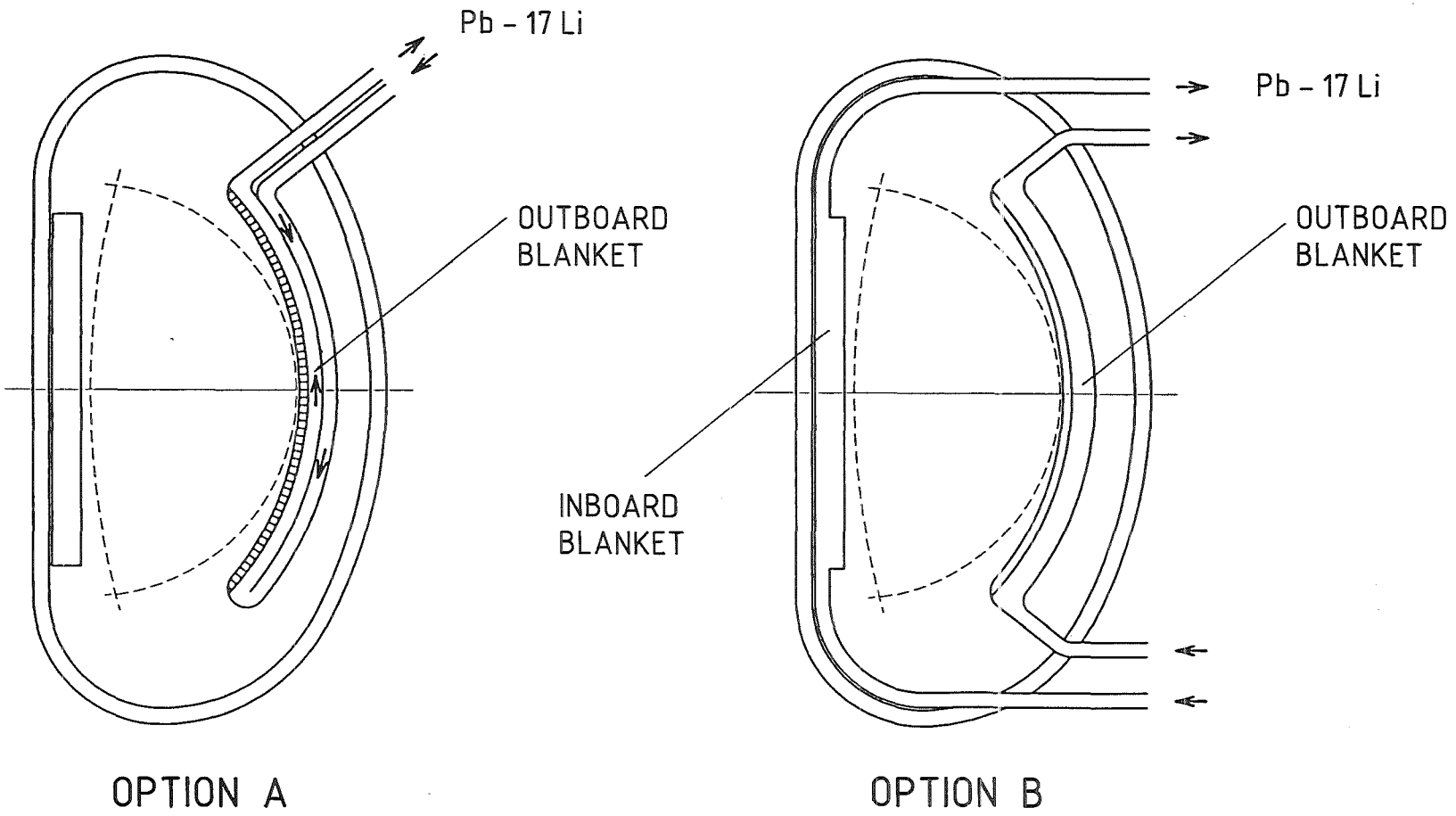

Figure 1: Schematic representation of concept variants of the self-cooled liquid metal blanket

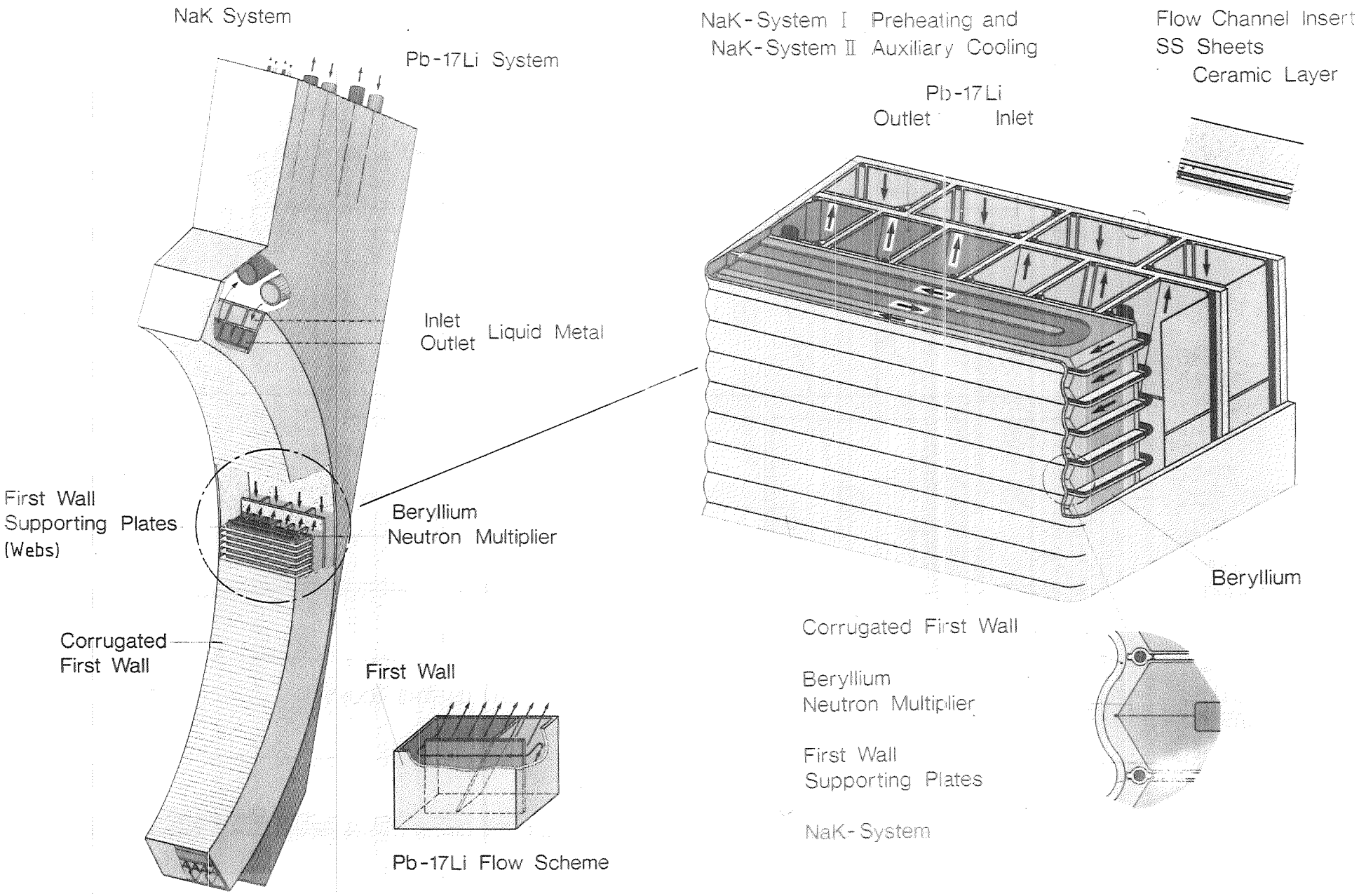

Figure 2: Structural design of a self-cooled liquid metal blanket; option A

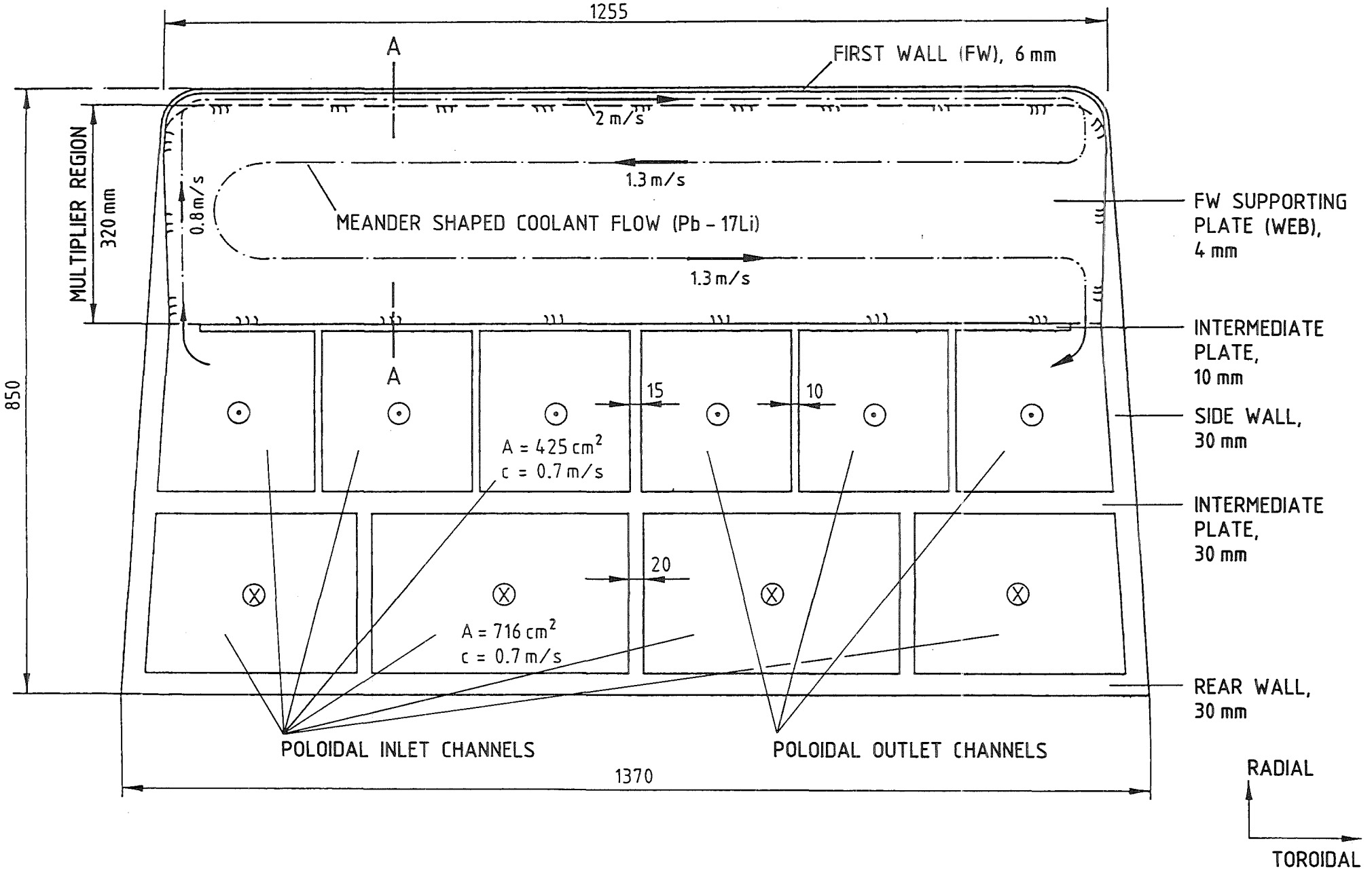

Figure 3: Equatorial blanket cross-section

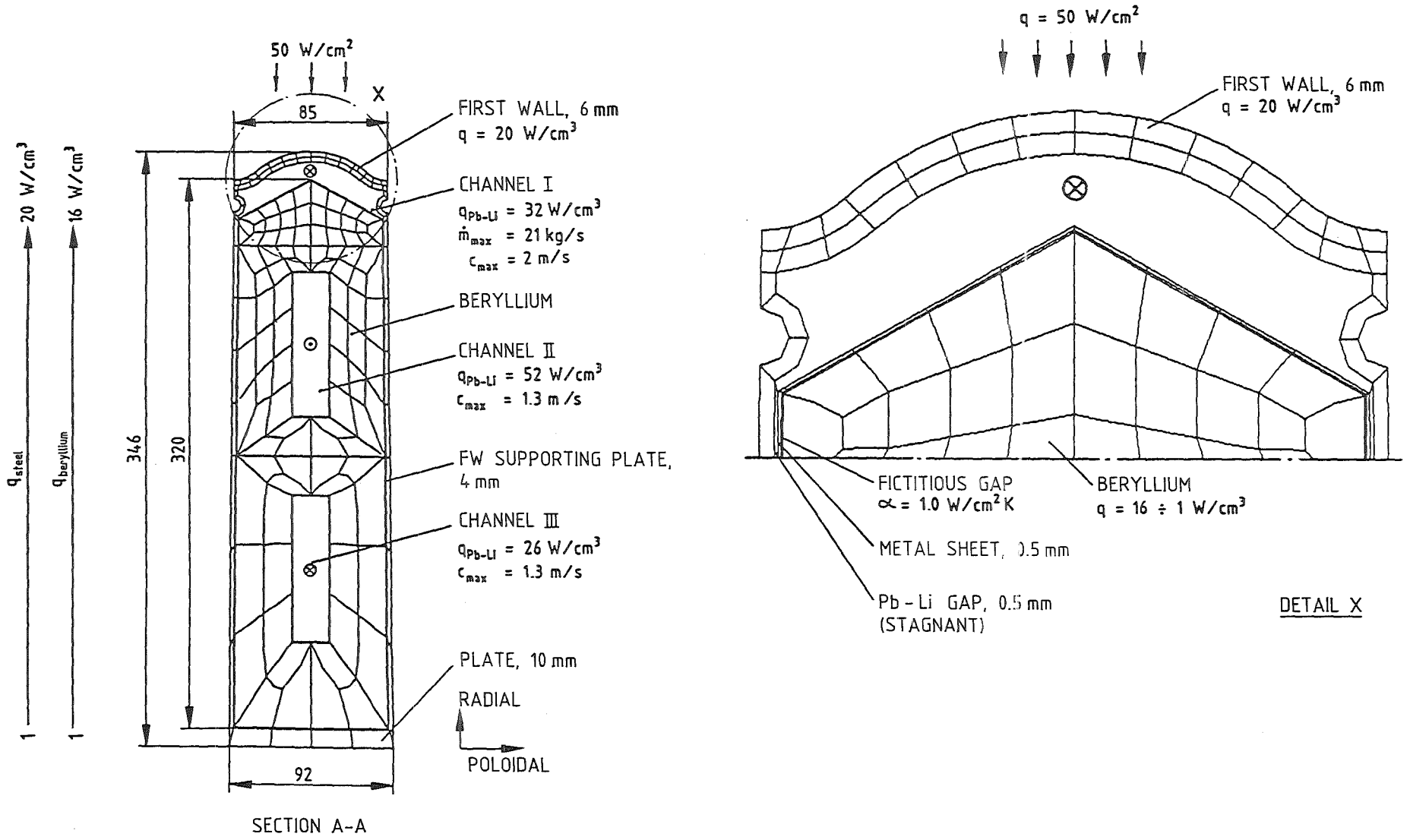

Figure 4: Cross-section of the multiplier region according to Figure 3; computer readable respresentation

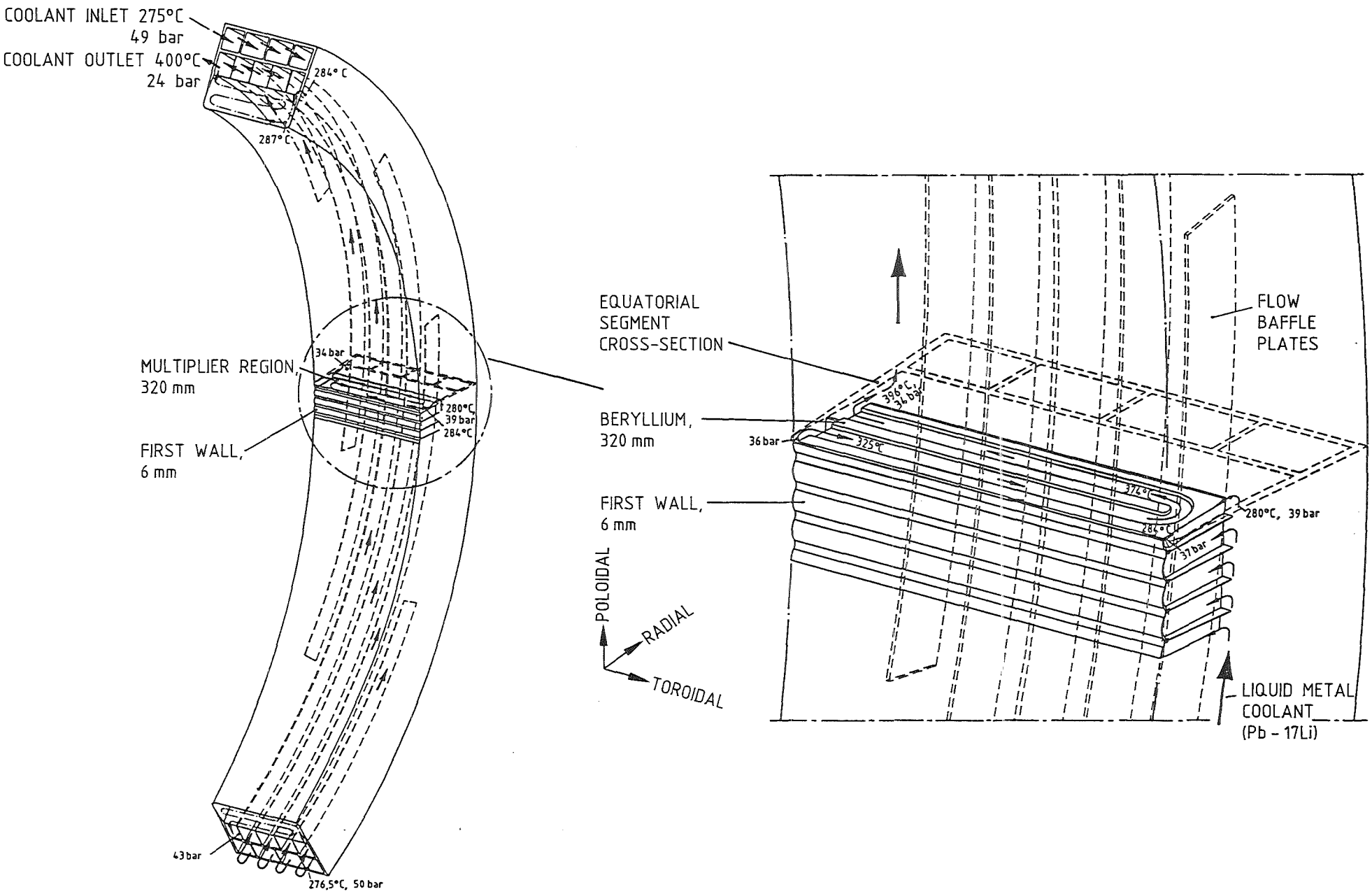

Figure 5: Global coolant temperature and coolant pressure distribution in the blanket; pump provided at high level

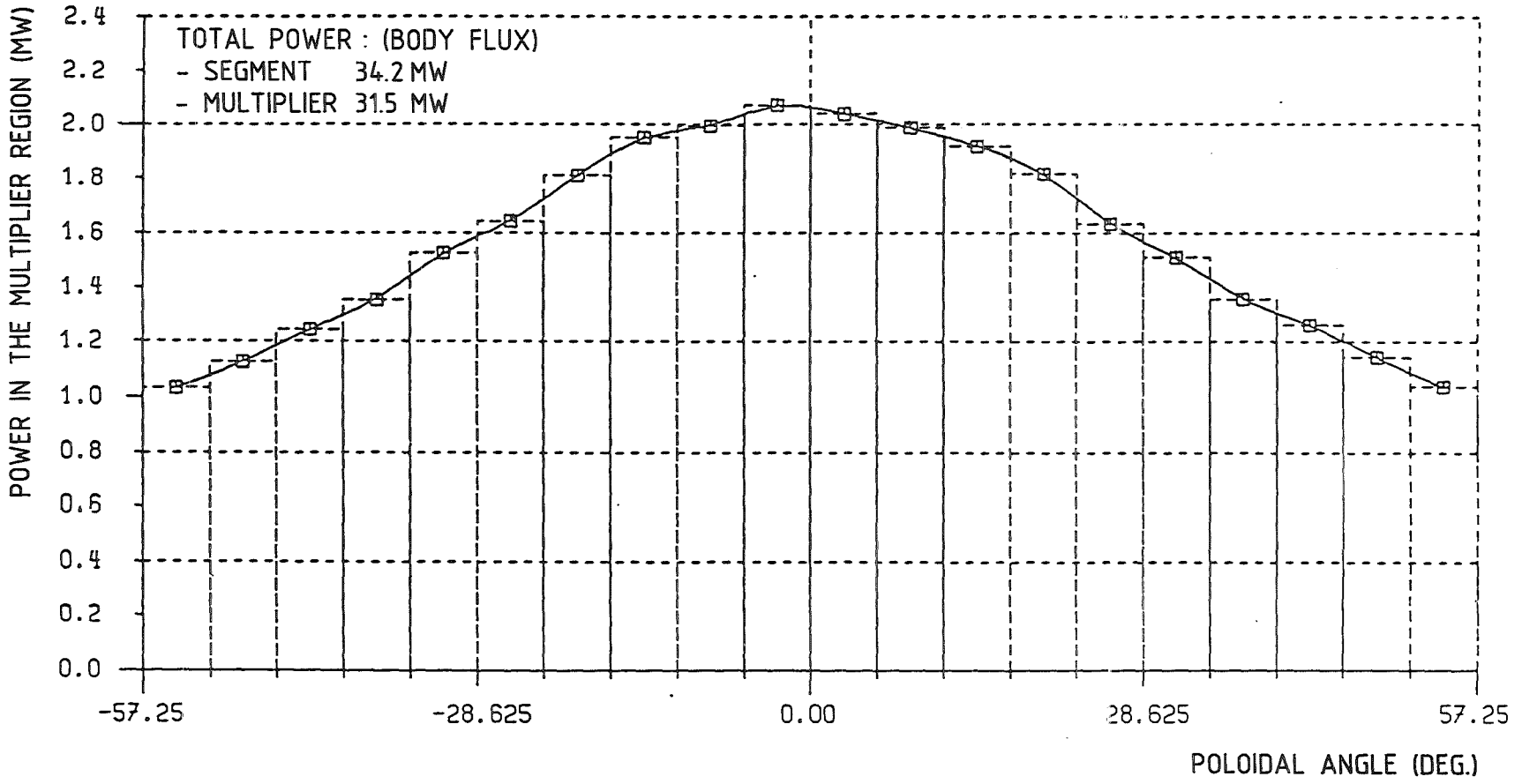

Figure 6: Poloidal power distribution in the front blanket part (multiplier region)

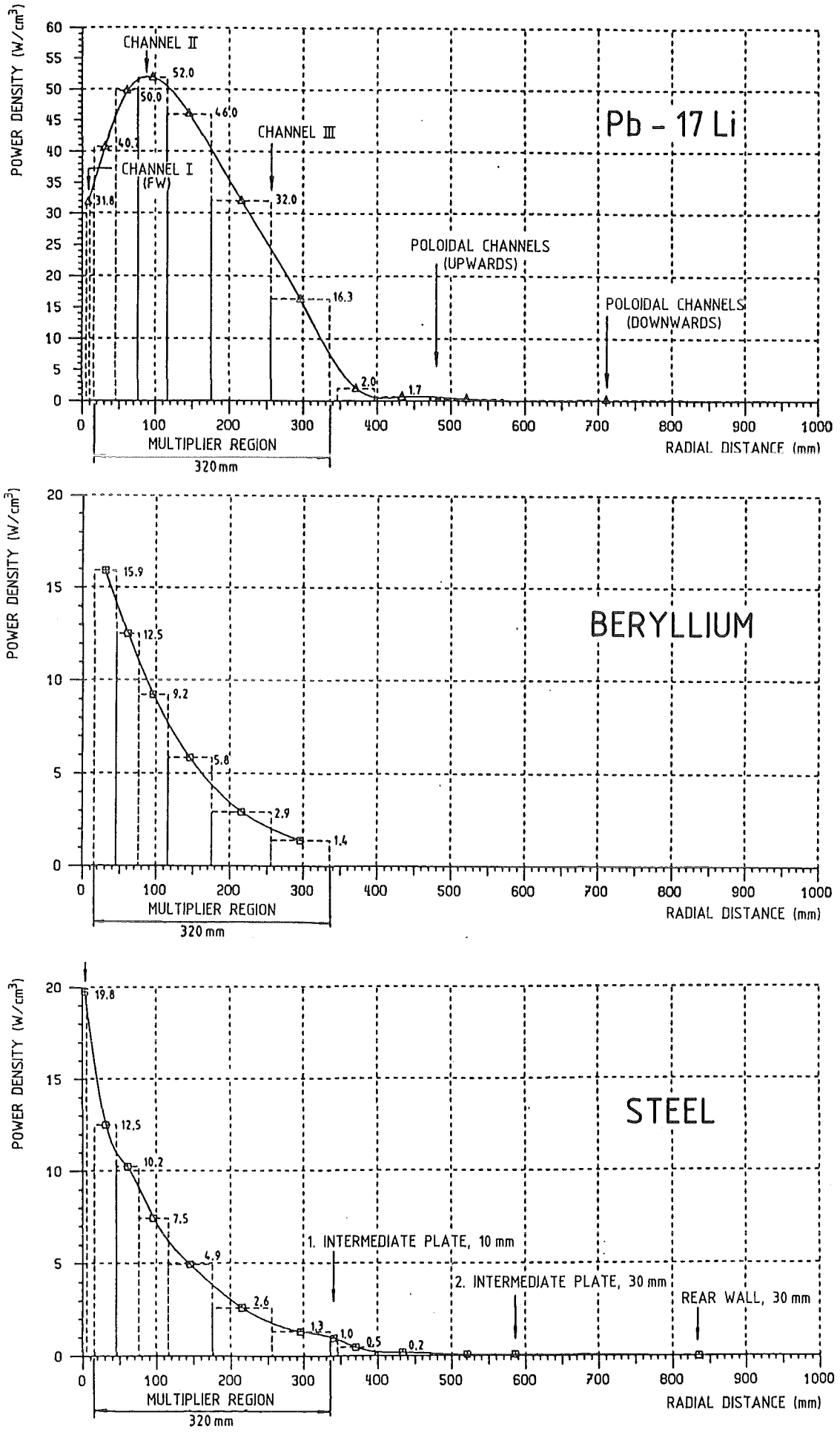

Figure 7: Radial distribution of the power density in the middle zone of the blanket

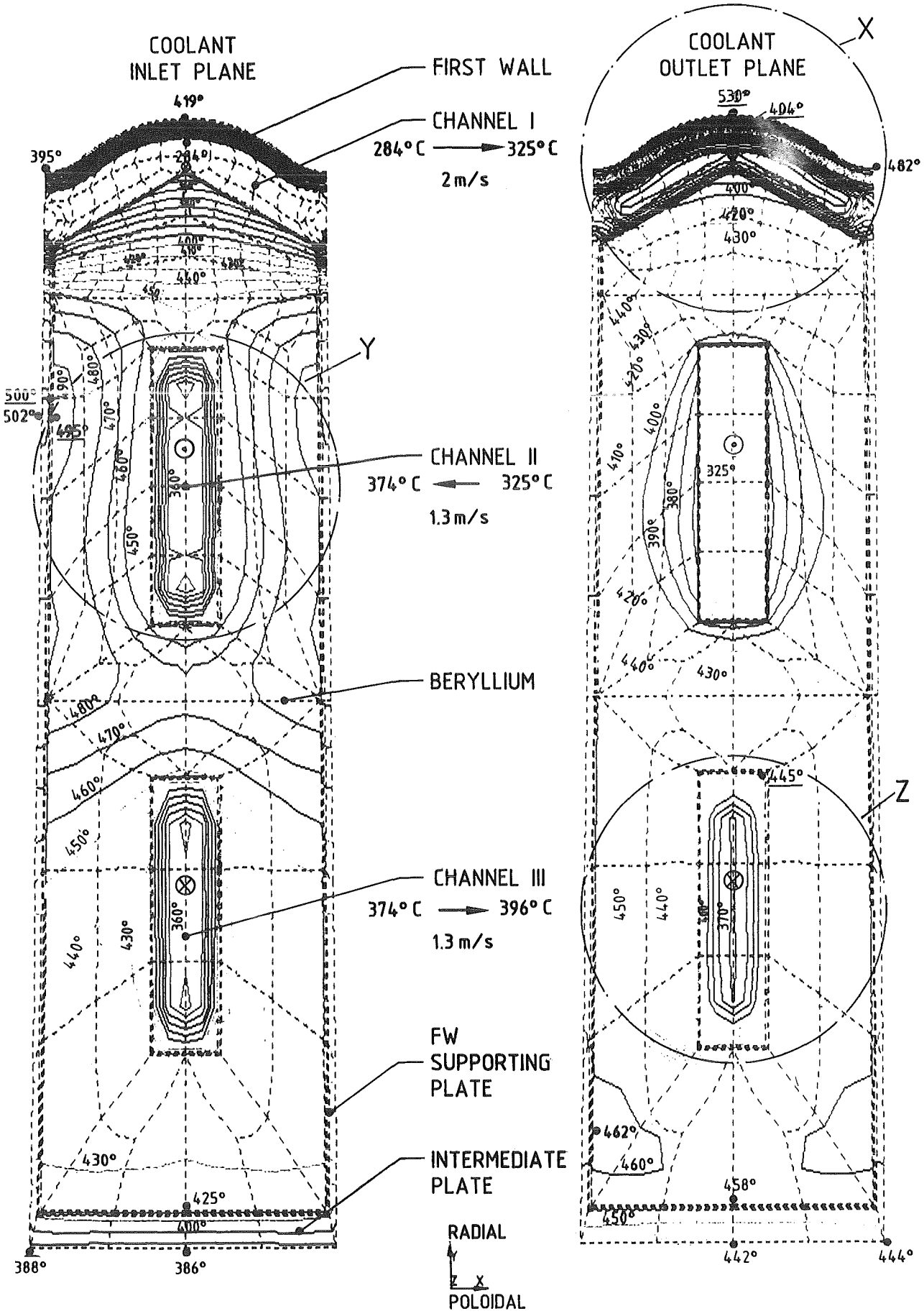

Figure 8: Temperature distribution in the multiplier region in the center of the blanket

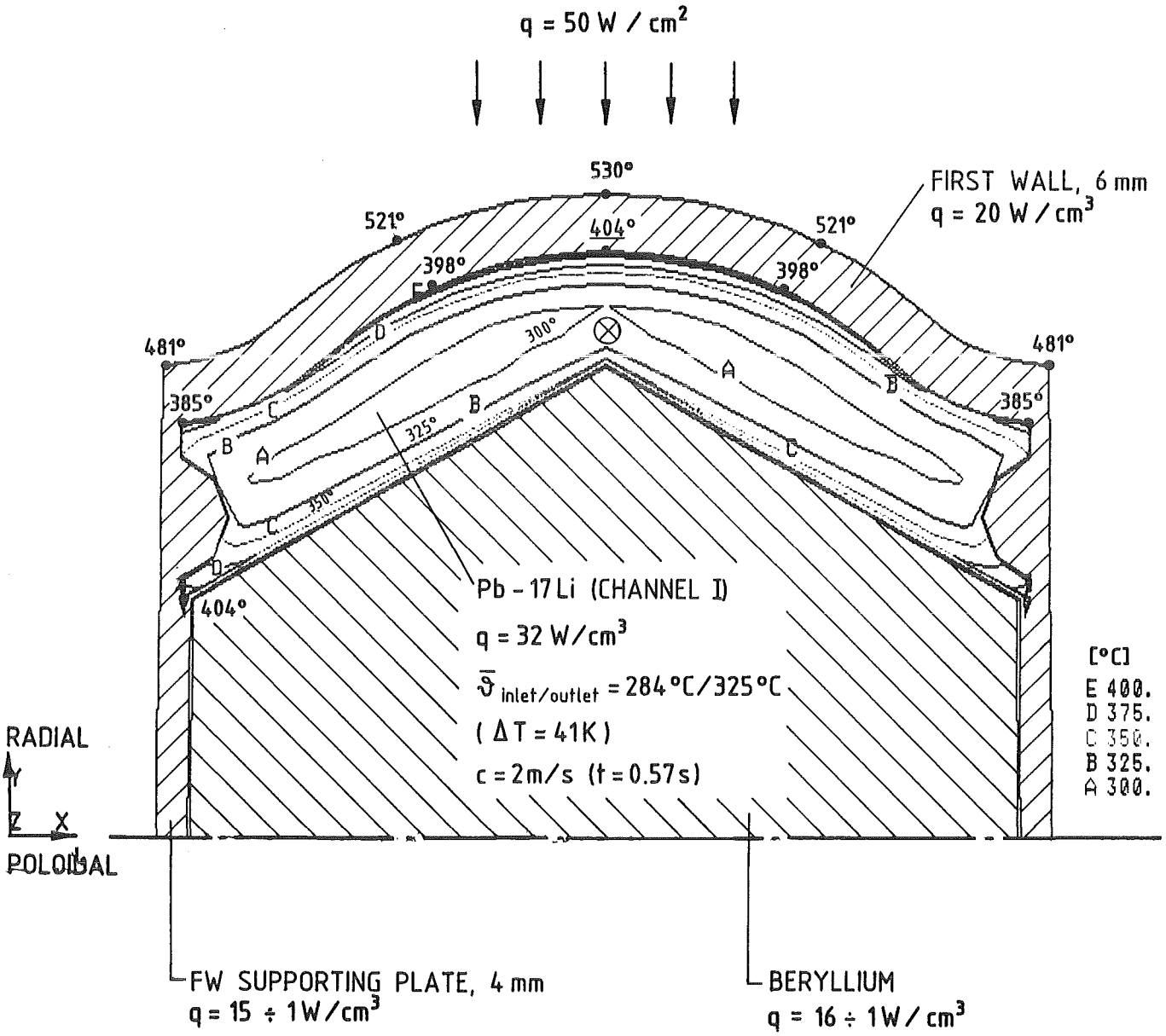

Figure 9: Coolant temperature distribution at the end of first wall coolant channel I in the center of the blanket according to Figure 8, detail X.

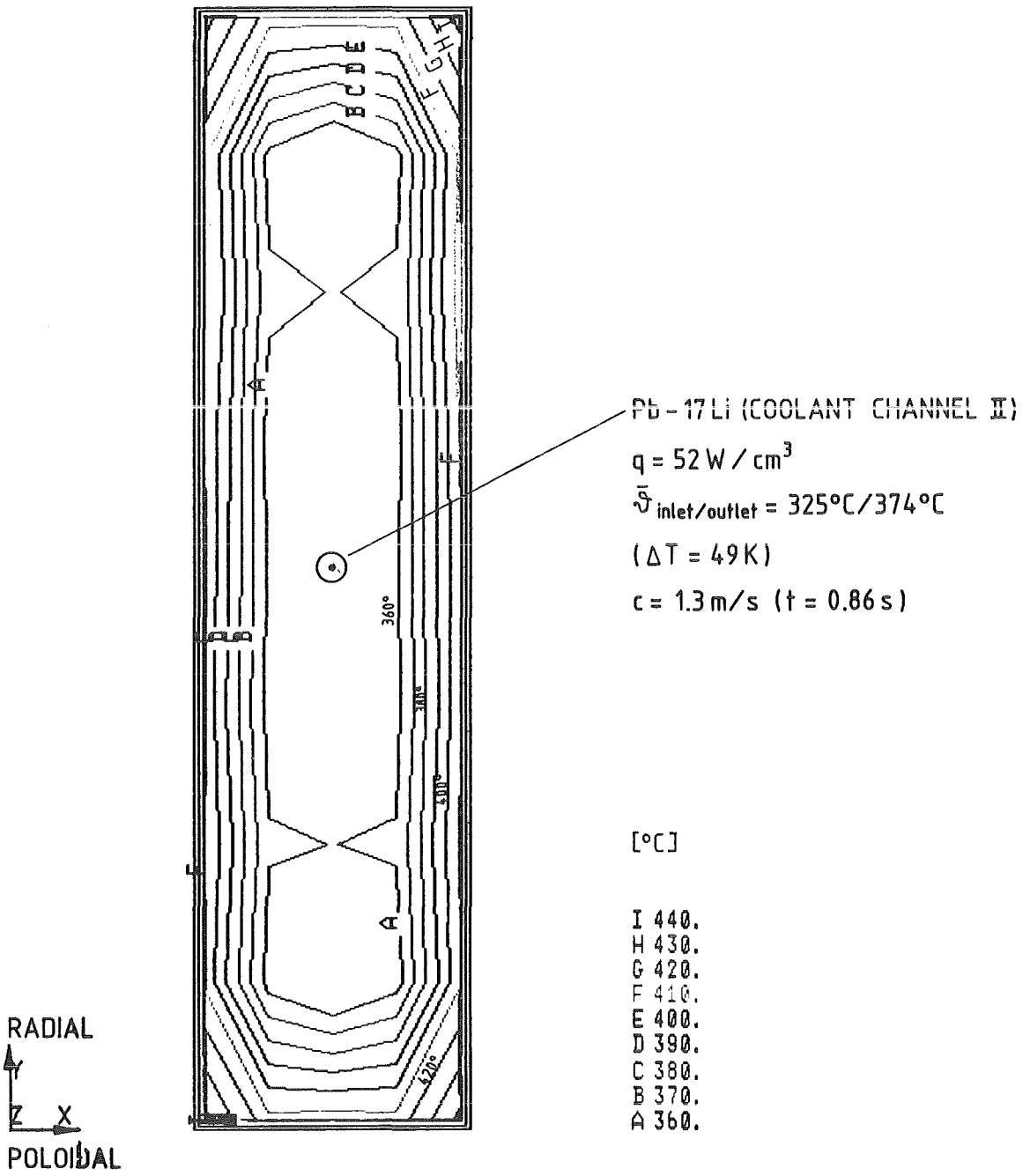

Figure 10: Coolant temperature distribution at the end of the beryllium coolant channel II in the center of the blanket according to Figure 8; detail Y

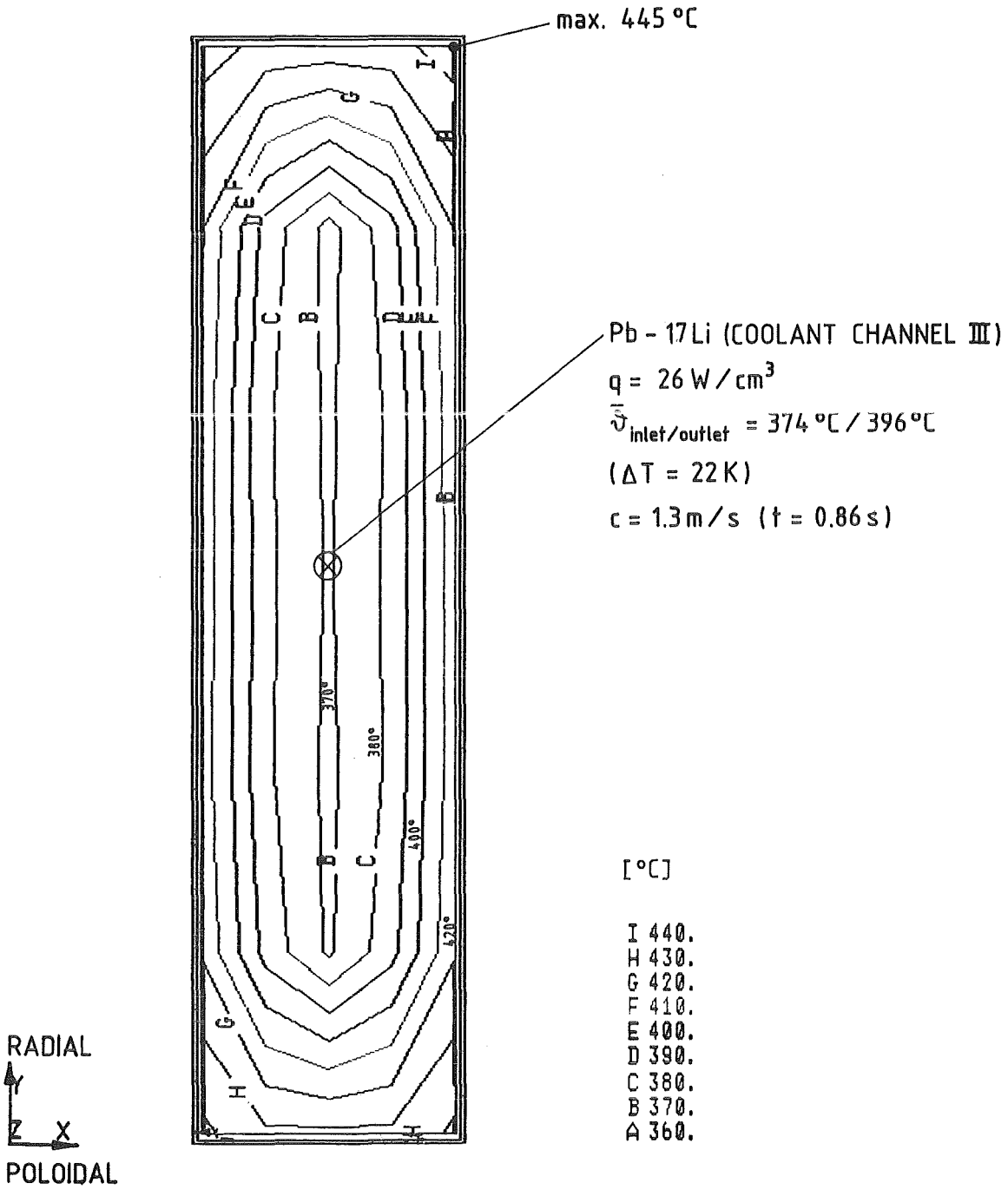

Figure 11: Coolant temperature distribution at the outlet of the beryllium coolant channel III in the center of the blanket according to Figure 8; detail Z

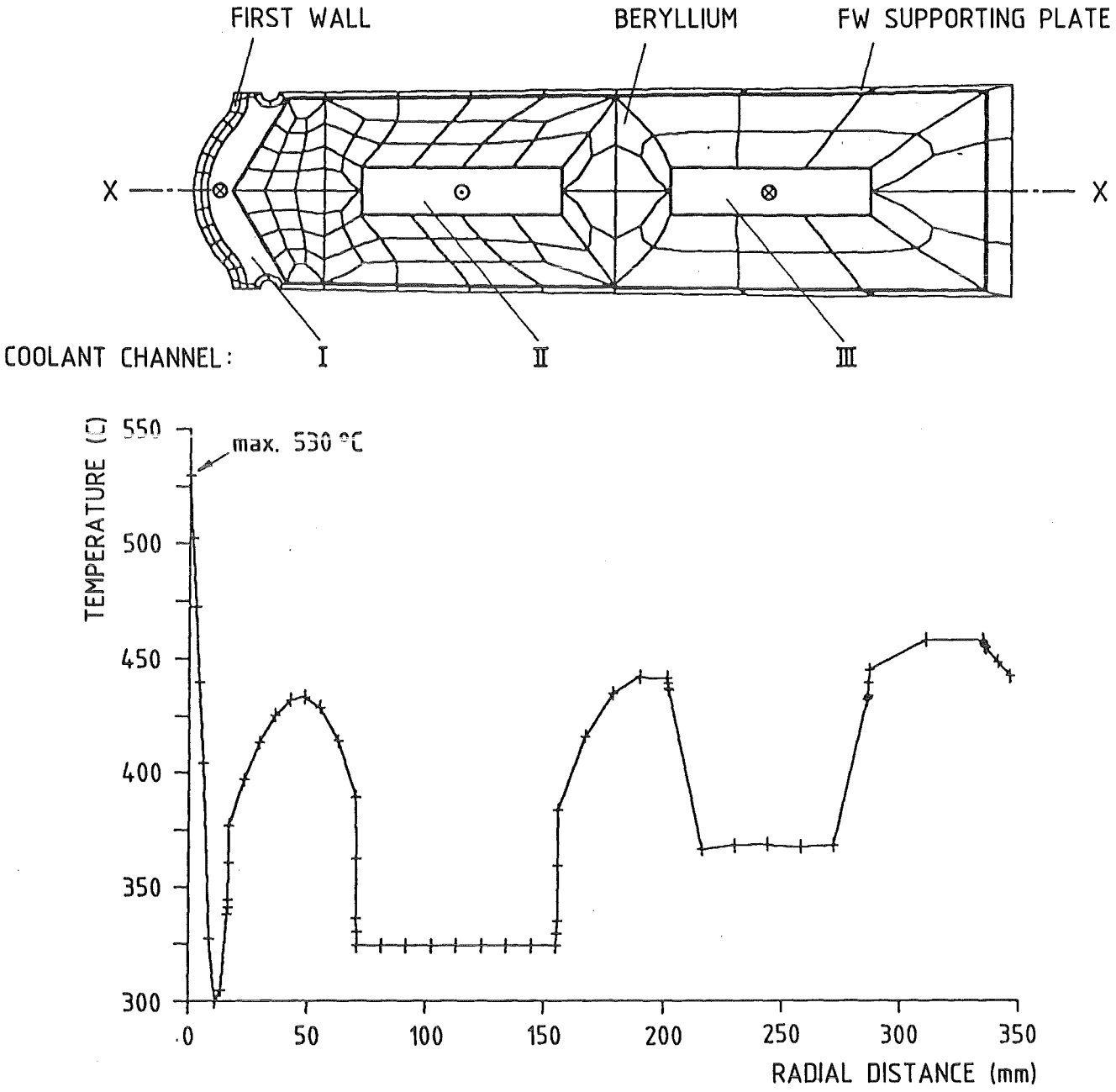

Figure 12: Radial temperature plot within the multiplier region (section X-X) at the coolant outlet plane in the center of the blanket

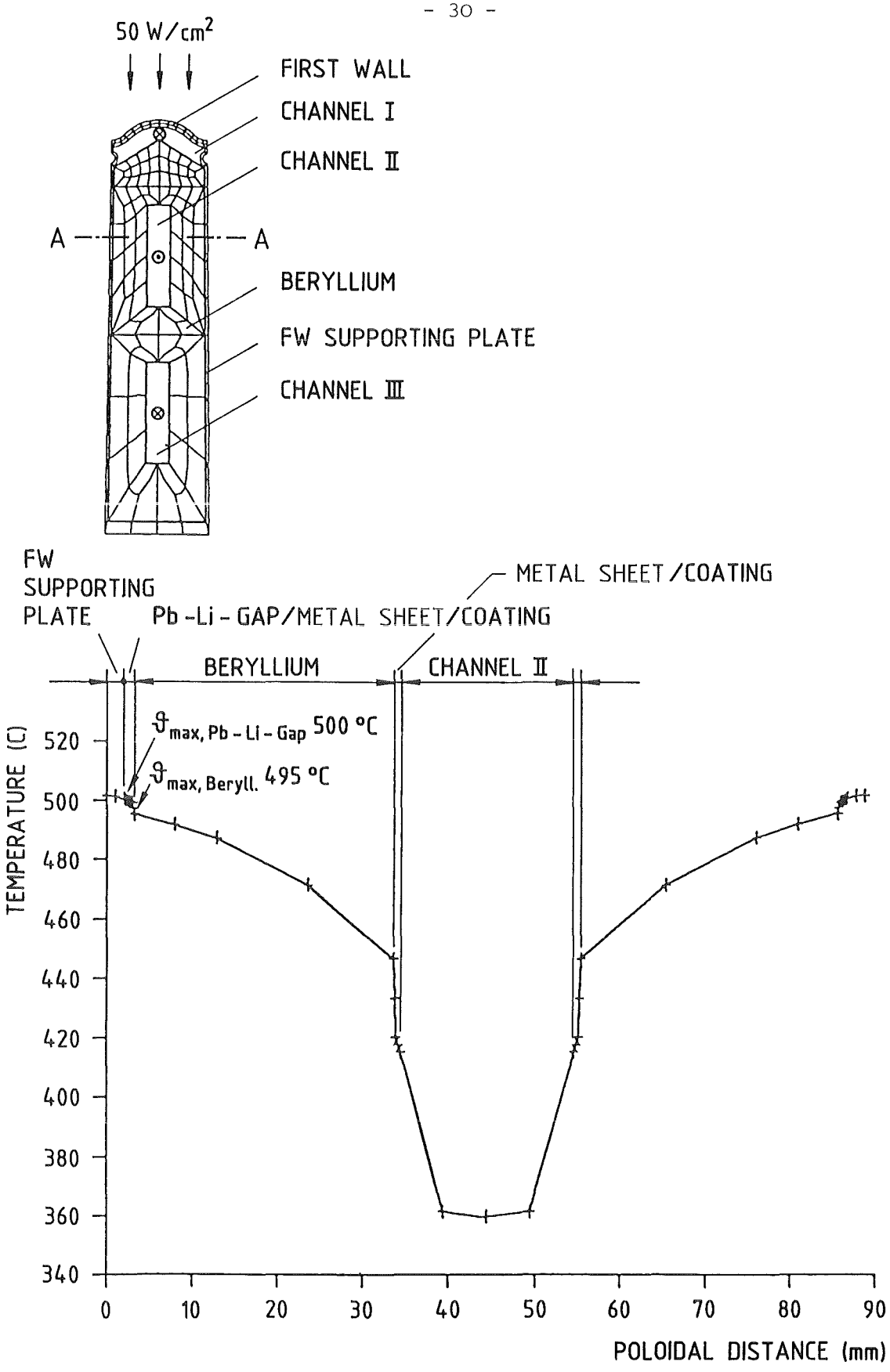

Figure 13: Poloidal temperature plot within the multiplier region (section A-A) at the coolant inlet plane in the center of the blanket

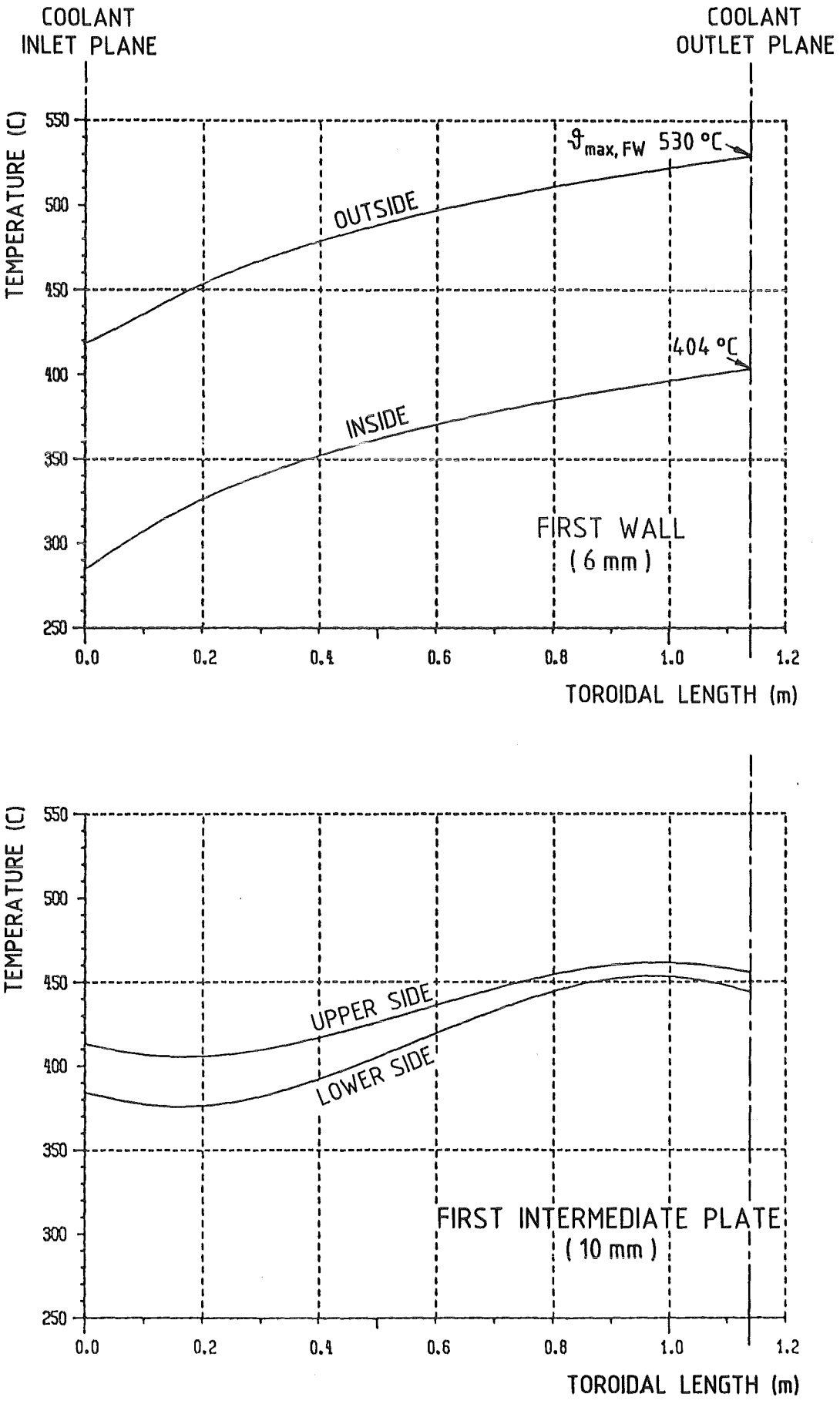

Figure 14: Toroidal temperature plot in the first wall and in the intermediate plate within the coolant channel length (without side wall regions)

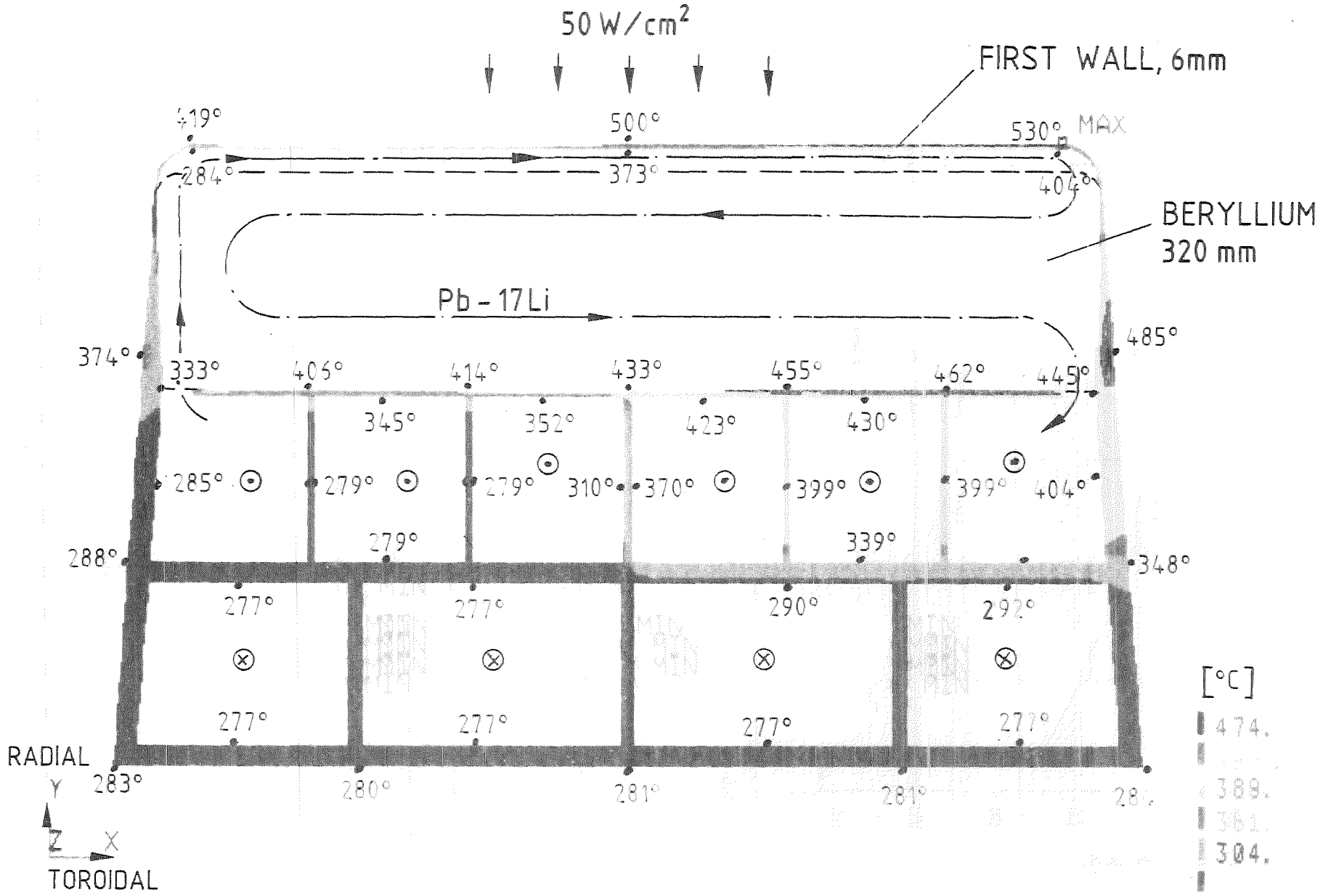

Figure 15: Temperature distribution at the equatorial plane of the blanket box

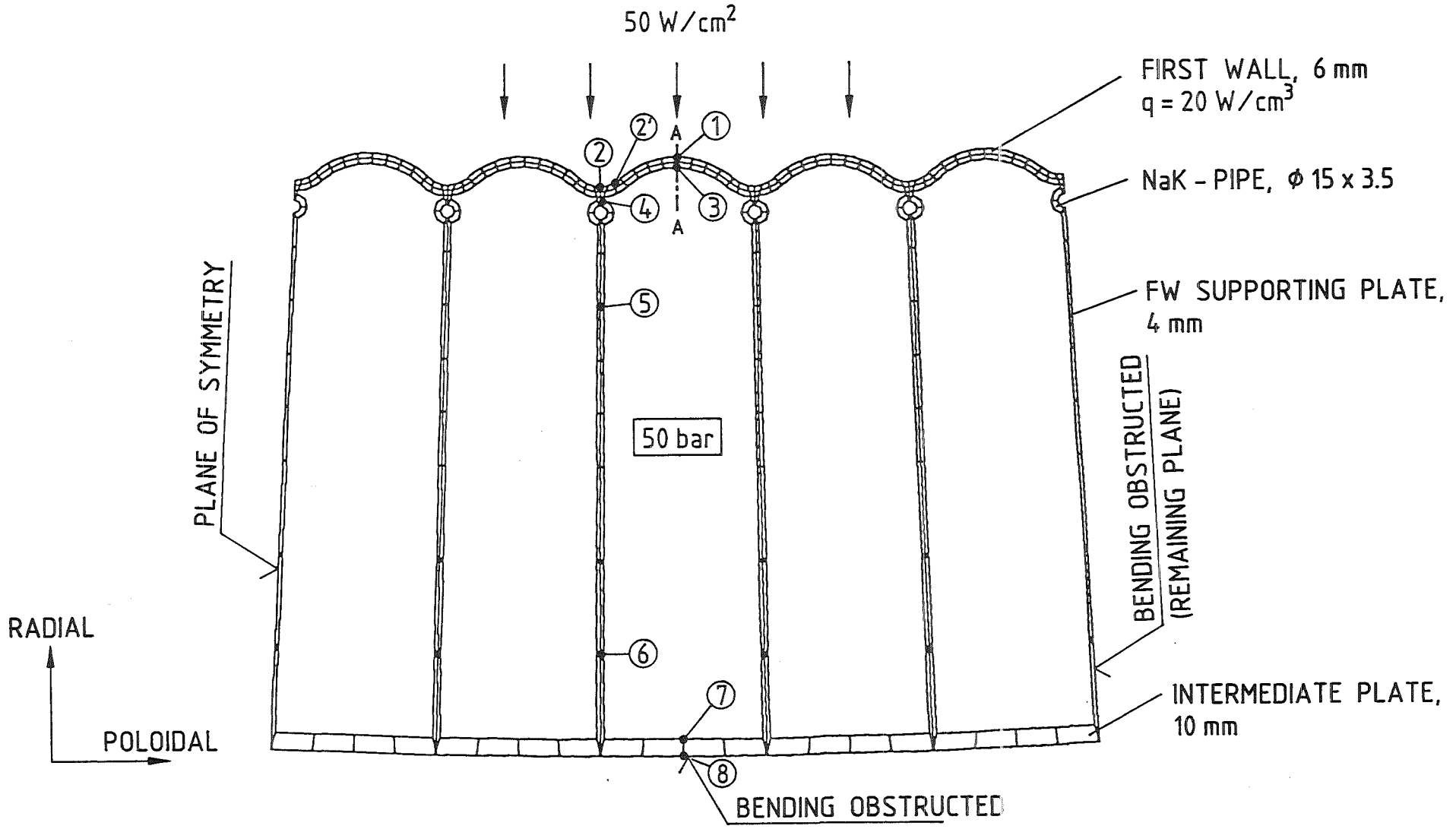

Figure 16: Finite element model of blanket front structure for stress analysis

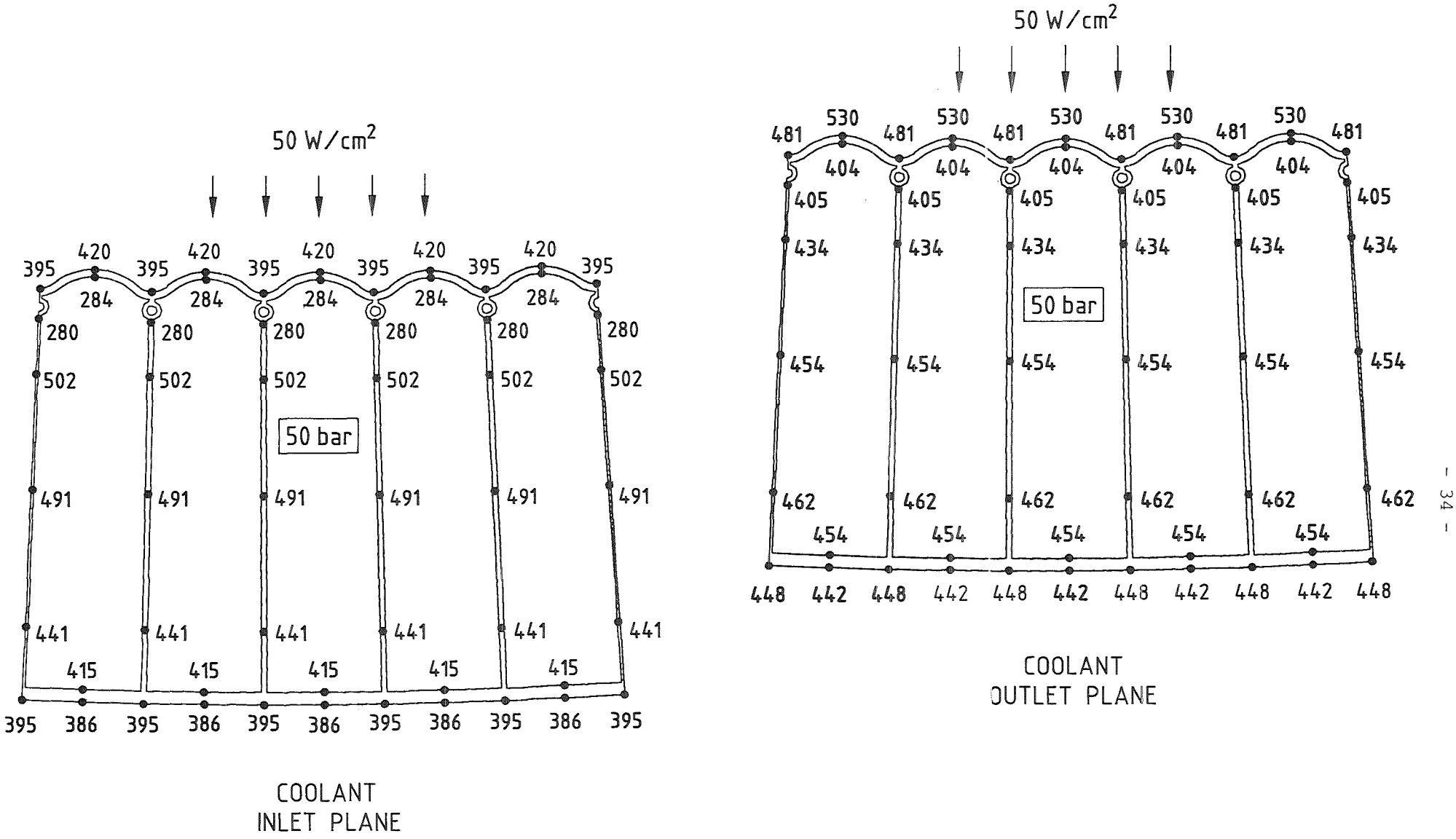

Figure 17: Temperature distribution in the blanket front structure in the center of the torus

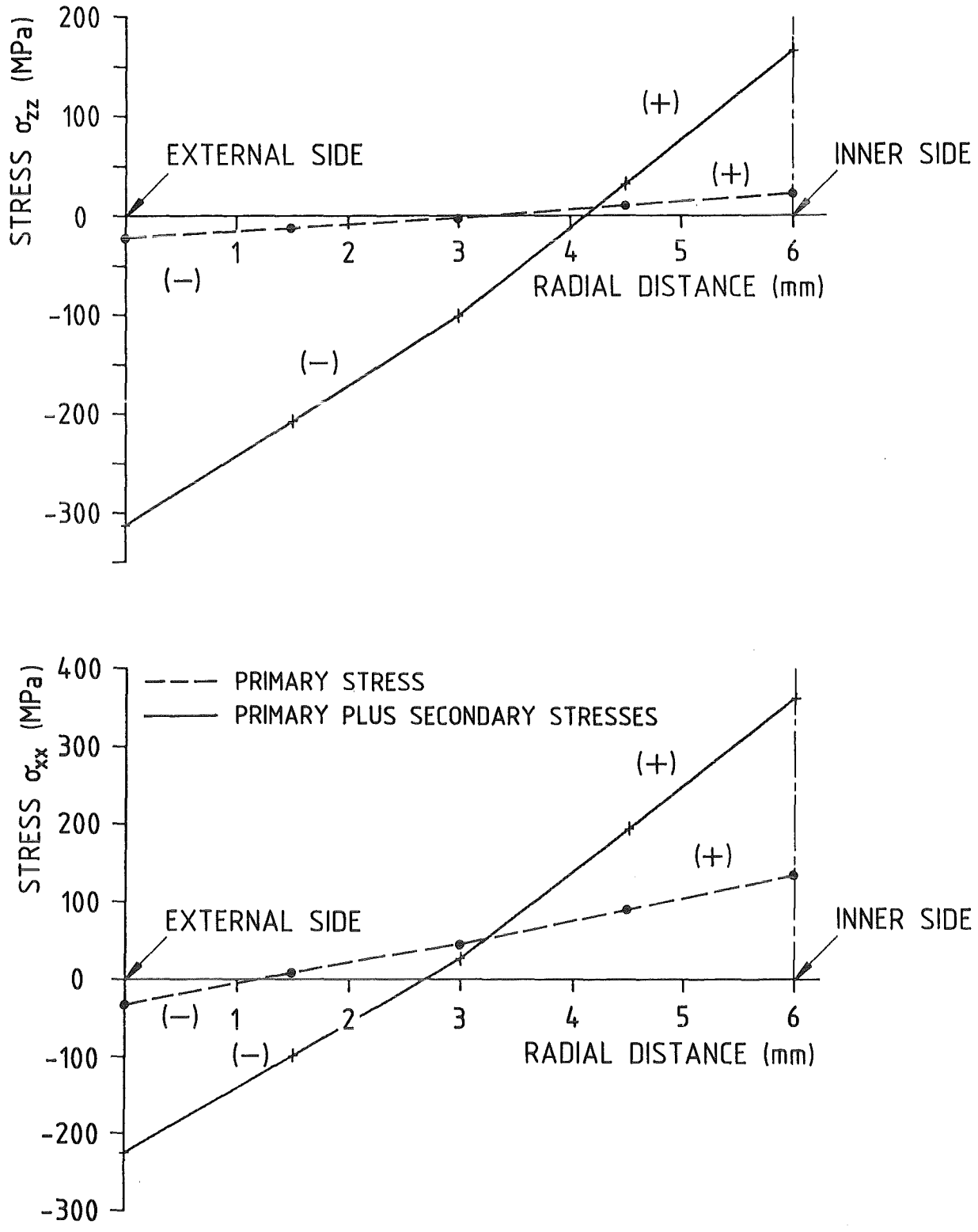

Figure 18: Development of normal stress σ_{xx} and σ_{zz} in the first wall region exposed to maximum thermal load (section A-A, Figure 16), directions: x ≙ poloidal, z ≙ toroidal

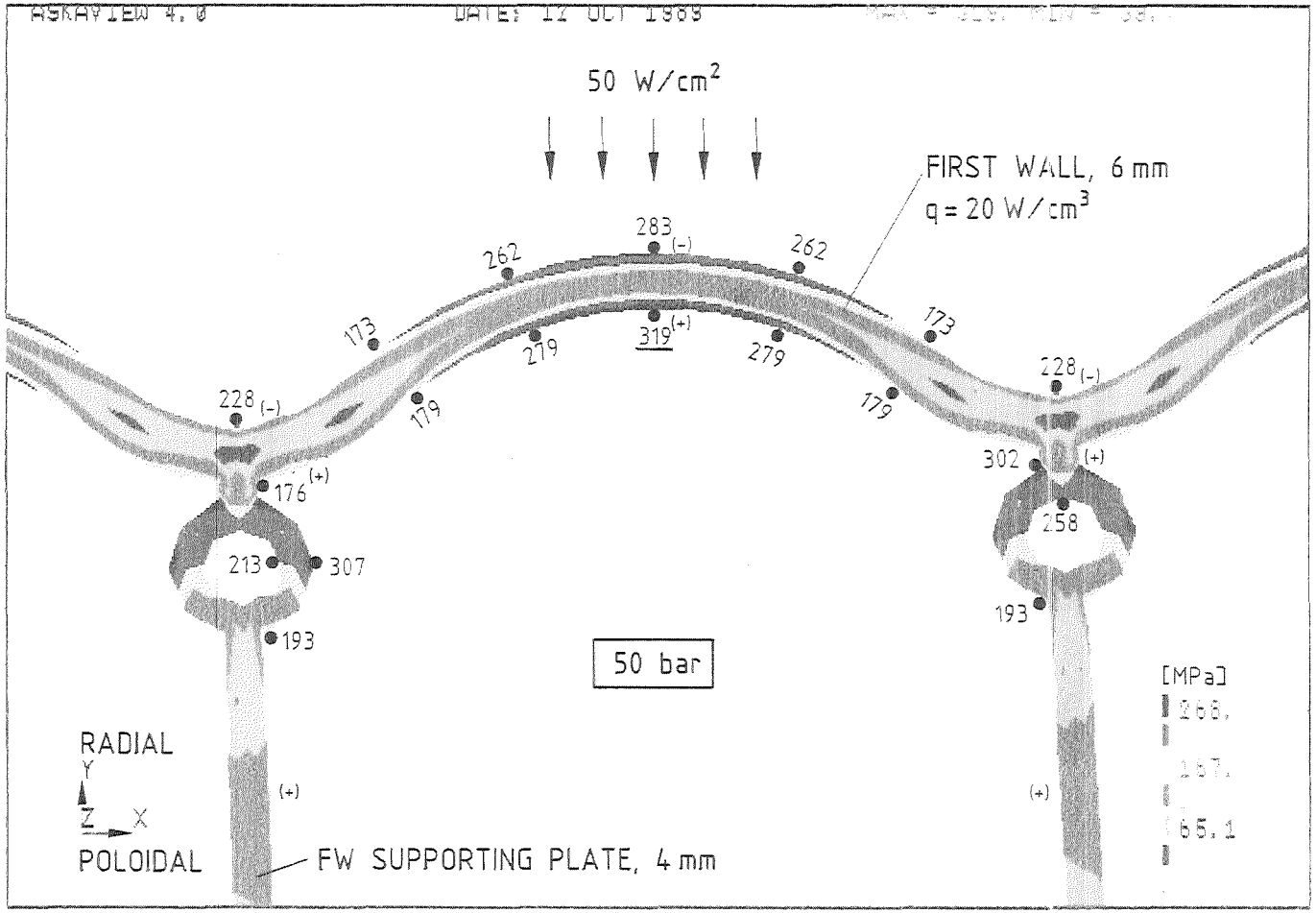

Figure 19: Von Mises primary stress plus secondary equivalent stresses in the first wall region exposed to maximum thermal load in the center of the blanket (coolant outlet plane)